Earthquakes and Structures, *Vol. 10, No. 6 (2016) 1291-1314*
DOI: http://dx.doi.org/10.12989/eas.2016.10.6.1291

Experimental fragility functions for exterior deficient RC beam-column connections before and after rehabilitation

Comingstarful Marthong[*1], Sajal K. Deb[2a] and Anjan Dutta[2b]

[1]*Department of Civil Engineering, National Institute of Technology Meghalaya, India*
[2]*Department of Civil Engineering, Indian Institute of Technology Guwahati, India*

(Received January 13, 2016, Revised April 21, 2016, Accepted May 2, 2016)

Abstract. The paper presents the development of experimental fragility functions for exterior RC beam-column connections based on results obtained from extensive testing carried out in the present study. Three typical types of seismically deficient beam-column connections, which are commonly prevalent in Indian sub-continent, were considered. These specimens were tested under cyclic displacement histories with different characteristics to induce different damage states. Rehabilitation specific fragility functions for damaged specimens were developed considering drift angle as a demand parameter. Four probability distributions were fit to the data and suitability of each distribution was evaluated using standard statistical method. Specimens with different damage states were rehabilitated appropriately and rehabilitated specimens were tested under similar displacement histories. Fragility functions for rehabilitated specimens have also been developed following similar procedure. Comparison of fragility functions for both original and rehabilitated specimens for each rehabilitation method showed close agreement, which establishes the effectiveness of the adopted rehabilitation strategies and hence would provide confidence in field application.

Keywords: fragility functions; beam-column connections; damage states; demand parameter; rehabilitation; cyclic loading

1. Introduction

Fragility functions is defined as the probability that some limit state is reached or exceeded for a given engineering demand parameter. One of the simplest methods of obtaining fragility functions is to use expert opinion. The most systematic study using this method is conducted by ATC-13 (1985). Other ways of obtaining fragility functions is to observe the actual post-earthquake structural damage or to use experimental data. However, in the absence of experimental or observational data as well as expert opinion, investigation of structural vulnerability is also done by adopting analytical methods. Further, fragility functions are commonly used in performance-based earthquake engineering for predicting the damage state of a

*Corresponding author, Assistant Professor, E-mail: commarthong@nitm.ac.in
[a]Professor, E-mail: skdeb@iitg.ernet.in
[b]Professor, E-mail: adutta@iitg.ernet.in

http://www.techno-press.com/journals/eas&subpage=7 ISSN: 2092-7614 (Print), 2092-7622 (Online)

structure subjected to an earthquake. Following different procedures and methodologies seismic fragility functions have been developed by many researchers. Based on the damage data used in the formulation the fragility functions can be broadly classified into three groups; heuristic, empirical and analytical fragilities (Ramamoorthy 2006).

(a) Heuristic fragility functions are developed based on the estimates of the probable damage distribution of building when subjected to different earthquake intensities provided by the civil engineers. The probability density functions are then fit to these damage estimates. Fragility functions are then obtained from the probability distributions of the damage states at each intensity level. The vulnerability assessment method prescribed in ATC-13 (1985) and ATC-40 (1996) is based predominately on expert opinion.

(b) In the empirical method the fragility functions are developed using the observed damage data from past earthquake events. Fragility curves are developed by integrating the damage with the ground motion intensity parameter. Yamazaki and Murao (2000) developed fragility functions for Japanese buildings using the damage data from the 1995 Kobe Earthquake.

(c) Analytical fragility functions are developed using the simulated response data obtained by time history analysis of simplified structural models of buildings for actual or synthetic earthquake ground motions. Singhal and Kiremidjian (1996) and Mosalam *et al.* (1997) developed analytical fragility functions for RC frame buildings.

Past studies on rehabilitation specific fragility function of structural components were very limited. Some of the important past researches where components fragility functions have been developed are summarized in this section. Shinozuka *et al.* (2002) developed analytical fragility curves for bridges retrofitted by column jacketing considering lognormal distribution as a function of peak ground acceleration (PGA). The improvement in the fragility with steel jacketing was quantified by comparing fragility curves of the bridge before and after column retrofit and it showed excellent improvement after retrofit. Aslani and Miranda (2005) developed fragility functions for slab-column connections to estimate the probability of experiencing different damage states. Damage states were defined based on previous experimental studies and linked with the rehabilitation method suggested by FEMA 308 (1998). Pagni *et al.* (2006) developed fragility functions for predicting the method of rehabilitation for older beam-column joints subjected to earthquake loading. Relations between damage states and engineering demand parameters (EDPs) were developed based on the previous studies reported in literature. Comprehensive procedures for creating fragility functions from various kinds of data were introduced by Porter *et al.* (2007a). Gulec *et al.* (2010) developed fragility functions for low aspect ratio reinforced concrete walls. Story drift was considered as the efficient response demand parameter. Defined damage states and rehabilitation methods were gathered from the past experimental data and expert opinion. Lignos *et al.* (2010) developed fragility functions to estimate the probability of exceeding different damage state in beam-to-column steel moment resisting frames. The response demand parameter was peak understory drift ratio. Experimental test results reported in the literature over past 14 years were used to develop the functions. Numerical simulation for developing fragility curves of a non-ductile reinforced concrete (RC) frames accounting different response characteristics such as (1) rigid joint, (2) inelastic joint shear response, (3) nonlinear joint shear response and anchorage failure, and (4) column shear failure were carried out by Jeon *et al.* (2015). The models developed employ an existing OpenSees materials and element formulations using large experimental data bases. Nonlinear dynamic analyses were performed using ground motions representative of the seismic hazard of California. They concluded that simulation of both joint and column shear failure is recommended for fragility assessment of non-ductile RC frames.

Literature review shows that though there are many ways to obtain fragility functions, development of fragility functions from experimental studies are considered to be the most reliable one among the different methods. However, there were a very few studies reported in the literature on development of experimental fragility function of structural components. Further, there was no experimental study reported in the literature on rehabilitation specific fragility functions of beam-column connection which has been validated after rehabilitation. Data-base on the behaviour of rehabilitated RC beam-column connections are well established e.g Filiatrault and Isabelle (1996), Karayannis *et al.* (1998), Tsonos (2001), Mukherjee and Joshi (2005), Karayannis *et al.* (2008a), Karayannis and Sirkelis (2008b), Alsayed *et al.* (2010), Hadi (2010), Marthong *et al.* (2013), Yurdakul and Avsar (2015), Marthong and Marthong (2016). The extent of damage on the specimen during testing is well dependent on the specimen types, loading sequence and displacement level adopted during testing and the ability to restore back the seismic capacity of the damaged specimen to the original level also depend on the adopted rehabilitation techniques. However, literature revealed that the mentioned parameters adopted by various researchers are not similar and varying depending on the availability of the test set-up and laboratory facilities. The extent of damage on the specimens is characterized by the damage states. Correct identification of damage states that linked with specific rehabilitation methods however depends on availability of correct information from literatures, written documents or published photographs etc. Therefore, in the present study, data generated from the experimental investigation of beam-column connections were used for the development of rehabilitation specific fragility functions of beam-column specimens both before and after rehabilitation.

Further, scanty information were reported on the damage states of beam-column connections with different deficiencies when subjected to cyclic loading having different characteristics. As the beam-column connections with beam weak in flexure, beam weak in shear and column weak in shear are quite commonly observed in many buildings in Indian sub-continent, it was considered to be appropriate to investigate the behaviour of these connections in the present study. Thus, the scope of the study was focussed on the development of experimental fragility functions based on the test results of forty two numbers of exterior RC beam-column connections comprising of specimens with different deficiencies and subjected to cyclic loading.

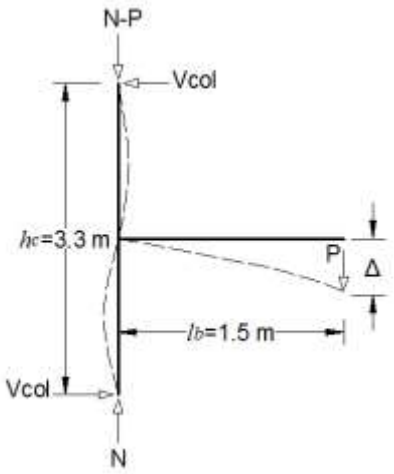

Fig. 1 Isolated exterior beam-column connection

2. Experimental program

2.1 Selection of specimens

The study was concentrated on an external isolated beam-column sub-assemblage as shown in Fig. 1. It comprised of half the length of column on each side of the joint and part of the beam up to mid-span, which corresponded to the points of contraflexure in beam and column under lateral loads. In Fig. 1, h_c is the story height, l_b corresponds to half beam span, N is the internal axial force in column, P is the beam-tip load, V_{col} is the column shear force and Δ is the vertical beam-tip displacement. Roller supports were provided at both the ends of column in order to maintain the symmetric boundary conditions for isolation of a single unit of beam-column connections. In this study, a typical full scale residential building with floor to floor height as 3.3 meters and the beam of 3.0 meters effective span was considered.

2.2 Description and casting of the specimens

The present study considered three types of typical full size connections, namely, (a) beam-column connections with beam weak in flexure (BWF), (b) beam-column connections with beam weak in shear (BWS) and (c) beam-column connections with column weak in shear (CWS). All these undamaged specimens were designated as control specimens. These control specimens were tested under cyclic displacement history and the damaged specimens were rehabilitated appropriately. The naming of the specimens was done with four alphabets. For example, BWFC stands for beam weak in flexure control specimen; similarly BWSC stands for beam weak in shear control specimens and CWSC stands for column weak in shear control specimens. The rehabilitated specimens were also named in line with the control specimens, e.g., BWFRe meaning beam weak in flexure rehabilitated specimen; BWSRe meaning beam weak in shear rehabilitated specimen and CWSRe meaning column weak in shear rehabilitated specimen. In each type, three geometrically similar specimens: full scaled (L), two third scaled (M) and one third scaled (S) were considered. Corresponding to three sizes, the specimens were named as BWFLC representing beam weak in flexure large control specimens. Similarly, BWSMC stands for beam weak in shear medium control specimens and CWSSC stands for column weak in shear small control specimens. The rehabilitated specimens were also named in line with the control specimens, e.g., BWFLRe meaning beam weak in flexure large rehabilitated specimen All the three dimensions (length, height and thickness) of two third and one third scaled specimens were arrived at by geometrically scaling down the dimensions of full scaled specimen. Similarly, reinforcement and coarse aggregates were also geometrically scaled down for satisfying the similitude requirement.

The BWF specimens were designed as under-reinforced beam following the provisions of IS: 456 (2000) and IS: 13920 (1993) for design and detailing. The specimens BWS were exactly similar in all respect to that of beam weak in flexure specimens except the spacing of shear reinforcement in beams. However, CWS specimens were cast with comparatively weaker grade of concrete than that used in earlier cases in order to make the column weak in shear. The cross section of the column was reduced while the cross section of beam was increased as compared to BWF and BWS. The main reinforcements in column were maintained similar to those of previous two cases, while same was increased in beam. Spacing for the lateral ties in the columns was increased to ensure the shear weakness of these specimens in column. The details of these specimens are presented in Table 1 and Fig. 2.

Table 1 Descriptions of beam-column connections

Specimen	Beam			Column			[a]Capacity ratio
	Span (mm)	Section (mm)	Longitudinal Reinforcement with yield strength 500 MPa	Length (mm)	Section (mm)	Longitudinal Reinforcement	
BWFLC	1500	300×360	2-ϕ20-top 2-ϕ20-bottom	3300	300×300	4-ϕ20	2.38
BWSLC	1500	300×360	2-ϕ20-top 2-ϕ20-bottom	3300	300×300	4-ϕ20	[b]$V_u<P_u$
CWSLC	1500	240×450	3-ϕ20-top 3-ϕ20-bottom	3300	240×300	4-ϕ20	0.99
BWFMC	1000	200×240	2-ϕ12+1-ϕ8-top 2-ϕ12+1-ϕ8-bottom	2200	200×200	4-ϕ12+2-ϕ8	2.36
BWSMC	1000	200×240	2-ϕ12+1-ϕ8-top 2-ϕ12+1-ϕ8-bottom	2200	200×200	4-ϕ12+2-ϕ8	[b]$V_u<P_u$
CWSMC	1000	160×300	3-ϕ12+1-ϕ8-top 3-ϕ12+1-ϕ8-bottom	2200	160×200	4-12ϕ+2-8ϕ	0.97
BWFSC	500	100×120	1-ϕ8+2-ϕ6-top 1-ϕ8+2-ϕ6-bottom	1100	100×100	2-ϕ8+4-ϕ6	2.31
BWSSC	500	100×120	1-8ϕ+2-6ϕ-top 1-8ϕ+2-6ϕ-bottom	1100	100×100	2-ϕ8+4-ϕ6	[b]$V_u<P_u$
CWSSC	500	80×150	2-ϕ8-top 2-ϕ8-bottom	1100	80×100	2-ϕ8+4-ϕ6	0.95

[a]ratio of ultimate moment capacity of columns framing into the joint to that of beam. Strong column-weak beam demands the capacity ratio as greater than 1.1 as per IS 13920-1993 and 1.2 as per ACI 318-08, 2008
[b]BWS specimens have same dimensions and longitudinal reinforcement as that of BWF except that the shear reinforcement provided in the beam are reduced to introduce shear weakness in beam. Capacity ratio for BWS specimens will be almost of similar order to those of BWF; but the capacity ratio will never be realized as failure load, V_u for BWS is lesser than the ultimate load carrying capacity, P_u of BWF specimens

Table 2 Test matrix of beam-column connections

Deficiency type	Loading Type-1	Loading Type-2	Loading Type-3
Beam Weak in Flexure (BWF)	BWFLC	BWFLC	BWFMC
	BWFMC	BWFMC	BWFMRe
	BWFSC	BWFSC	
	BWFLRe	BWFLRe	
	BWFMRe	BWFMRe	
	BWFSRe	BWFSRe	

Table 2 Continued

Deficiency type	Loading Type-1	Loading Type-2	Loading Type-3
Beam Weak in Shear (BWS)	BWSLC	BWSLC	BWSMC
	BWSMC	BWSMC	BWSMRe
	BWSSC	BWSSC	
	BWSLRe	BWSLRe	
	BWSMRe	BWSMRe	
	BWSSRe	BWSSRe	
Column Weak in Shear (CWS)	CWSLC	CWSLC	CWSMC
	CWSMC	CWSMC	CWSMRe
	CWSSC	CWSSC	
	CWSLRe	CWSLRe	
	CWSMRe	CWSMRe	
	CWSSRe	CWSSRe	

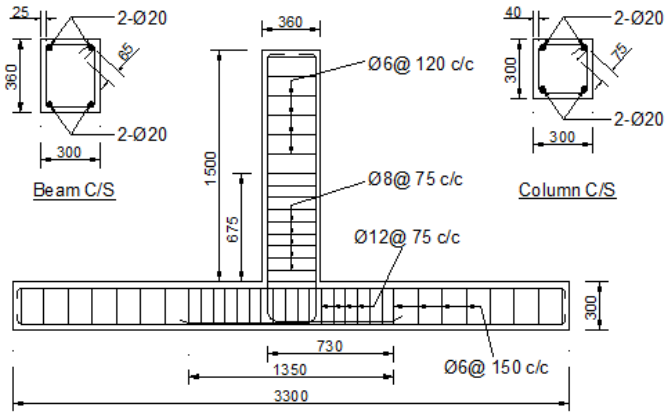

(a)

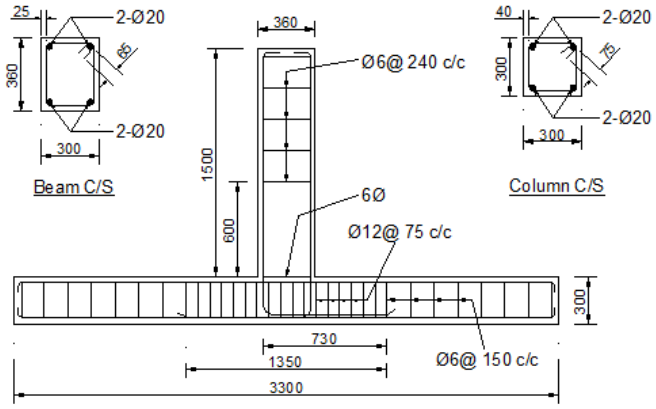

(b)

Fig. 2 Reinforcement details of beam-column connections (a) BWFLC (b) BWSLC (c) CWSLC
Note: All dimensions are in millimetres

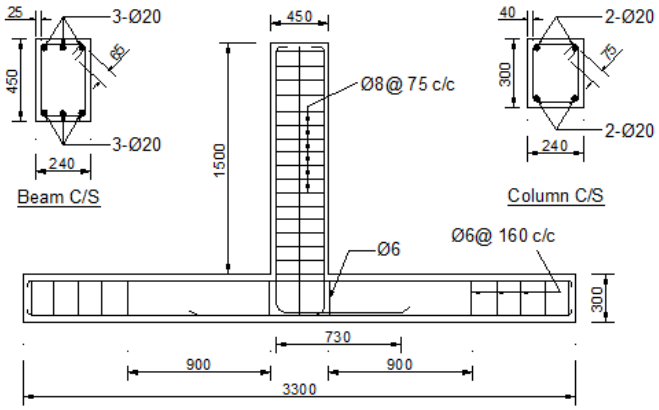

(c)

Fig. 2 Continued

Ordinary Portland cement (OPC) of 53 grades conforming to IS: 12269 (1987) was used in the construction of the test specimens. Natural sand confirming to Zone-II (IS: 10262, 2009) was used as fine aggregates. The maximum size of coarse aggregates used in concrete was limited to 16 mm. Aggregates used were tested as per relevant codes [IS: 2386 (a) and (b), 1963]. Concrete mix was designed for target cube strength of 30 N/mm^2 for beam-column connections with BWF and BWS, while a lower grade with target cube strength of 25 N/mm^2 was used for CWS specimens. The design mix proportion for the concrete used for BWF and BWS specimens was 1.00: 1.84: 3.18 (*cement: sand: coarse aggregate*) with water-cement ratio of 0.59, while same was 1: 2.26: 4.0 for CWS specimens with water-cement ratio of 0.65. The average compressive strength was obtained as 31.5 MPa from the cubes of BWF and BWS specimens, while the same was 25.3 MPa for CWS specimens. Reinforcing steel of diameters 20 mm, 12 mm and 8 mm were of High Yield Steel Deformed (HYSD, Fe 500) bar type, while reinforcing steel of diameters 6 mm was of mild steel (Fe 250) type. The steel bars have been tested as per provisions of IS: 432(I) (1982) and IS: 1608 (1995). The yield stress (MPa) and ultimate stress (MPa) for HYSD bars were 530 MPa and 620 MPa, while the same for Fe 250 bars were 285 MPa and 450 MPa respectively.

2.3 Test set-up and instrumentations

Typical schematic diagram of the set-up as shown in Fig. 3(a) was used for experimental investigation. Application of load was facilitated by Strong floor, Strong wall and *A*-frames available in the Dynamic Structural Testing Facility at IIT Guwahati. Servo hydraulic dynamic actuators (Make: MTS, USA) of capacity 250 kN having a maximum displacement range of ±125 mm was used for application of cyclic displacement histories. The column of the connection was placed in horizontal position while the beam was placed in vertical position in the set-up. An axial load of 10% of gross capacity of column was applied to the column to represent gravity load. The load on column was applied by a 500 kN capacity jack, which was properly calibrated. The jack was abutting against an *A*-frame, which was fabricated for the specified load carrying capacity. To simulate the support condition at both ends of the column, roller supports were fabricated by making grooves inside mild steel plates. The actual testing arrangement of the specimens is shown

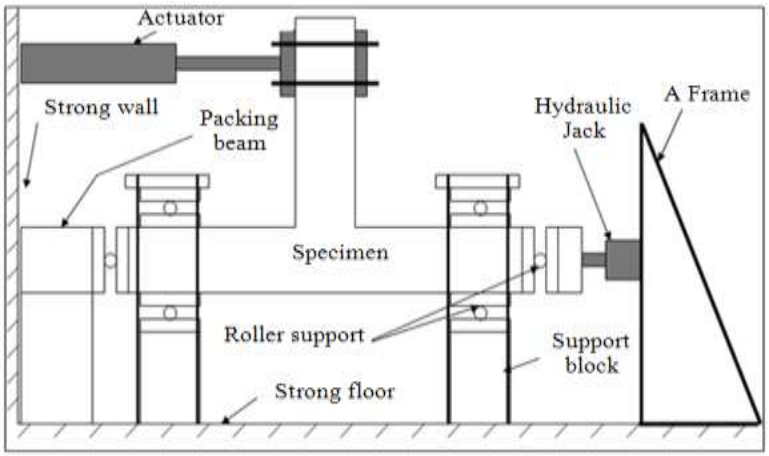

(a)

(b)

Fig. 3 (a) Schematic diagram of test set-up and (b) Actual testing arrangement

in Fig. 3(b). The MTS actuator was equipped with in-built load cell and linear-variable differential transformer (LVDT) for measuring actuator force and displacement respectively.The LVDT is coaxially mounted within the actuator piston rod. The controller can generate prescribed dynamic displacement or force for the actuator. The actuator is of double ended and double stroke nature.

2.4 Loading characteristics

The nature and extent of damage in a structure during earthquake depends on the characteristic of loading. Number of cycles in the displacement time history, frequency of excitation and the level of displacement amplitude are some of the parameters which contributes to the extent of damage in a specimen. Three typical loading types considered in this study are shown in Fig. 4. In loading type-1, each displacement amplitude was repeated for three cycles with loading frequency of 0.025 Hz, while only one cycle was used for each amplitude under loading type-2 with same loading frequency. Thus, numbers of cycles in the loading type-1 is much higher than that in the

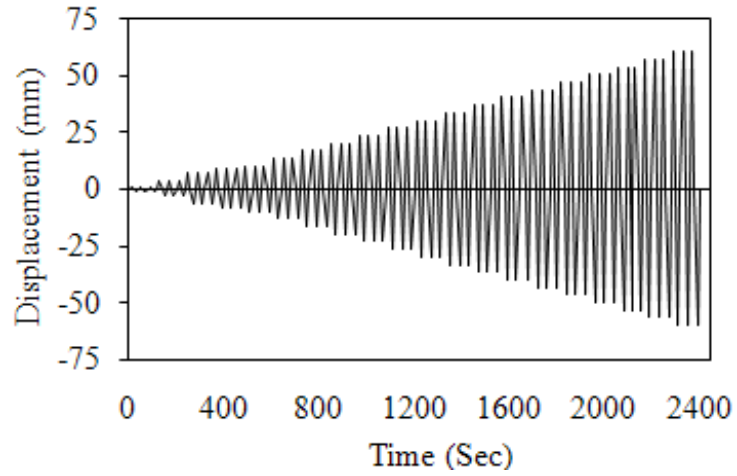

(a)

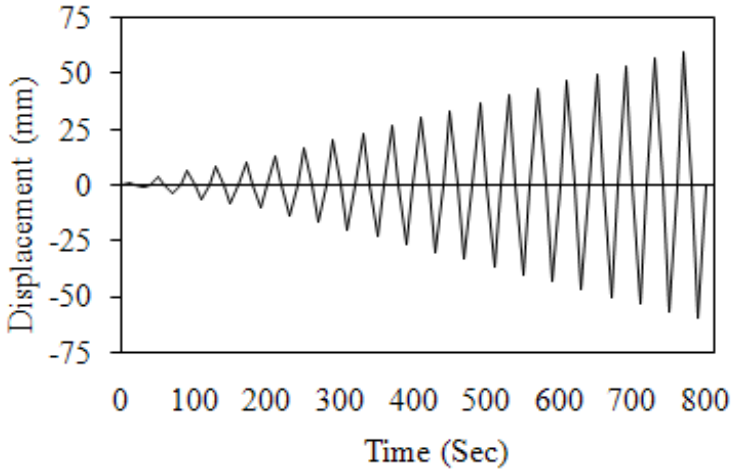

(b)

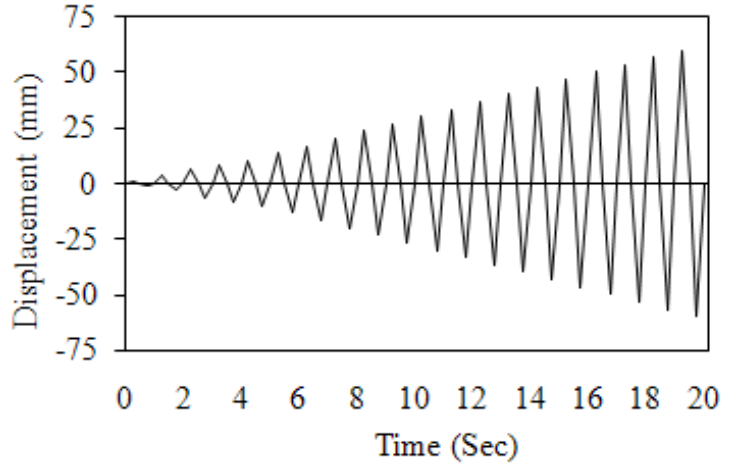

(c)

Fig. 4 Typical displacement history (a) Loading type-1 (b) Loading type-2 (c) Loading type-3

loading type-2. Therefore, it is expected that the loading type-1 will induce higher level of damage in the specimens compared to that induced by the loading type-2. The loading type-3 was similar to loading type -2; but with frequency of cyclic displacement as 1.0 Hz.

The importance of loading sequence effects has not yet been established through research and the sequence of large versus small excursions in an element of a structure subjected to a severe earthquake does not follow any consistent pattern (Karayannis and Sirkelis 2008b). In order to utilize results obtained from cyclic loading test on structural elements for a general performance evaluation, there is a need to establish loading history that captures the critical issues of the element capacity as well as the seismic demand. In the adopted loading type-2, emphasis was given on the large inelastic excursion since they cause large damage and could lead quickly to ultimate state. Thus in order to draw conclusions for the ultimate states, a loading program with constantly increasing displacement was chosen. Further, it is recognized that structures depend on a large number of variables and a unique loading history will always be a compromise. Thus to address this issue, multi-cycle loading history (loading type-1) was also adopted. Furthermore, most of the test conducted for RC beam-column connections are of quasi-static nature. Obviously, it is advantageous because the quasi-static cyclic testing allows a careful monitoring of the specimen behaviour during the test and the strain-rate effects do not affect the material behaviour. However, these frequencies are substantially lower than those corresponding to the actual seismic excitation. Thus, in order to address the same, higher loading frequency (loading type-3) was also adopted in the presented work.

The amplitude of the displacement histories as reported by Choudhury (2010) was adopted in this study. The amplitude of applied displacement in the case of full scaled specimens was ±1.44 mm, which corresponded to appearance of first crack in BWF. This was followed by displacement amplitude of ±5.00 mm, ±10.00 mm, ±12.50 mm and ±15.0 mm. Displacement amplitude of ±12.5 mm was chosen because at this displacement level yielding of steel was expected as per observation from numerical analysis of BWF. Amplitude of the displacement histories were scaled down for two-third and one-third scaled specimens respectively. Same sequence was maintained for other specimens as well. Different loading types were adopted in order to induce different extent of damages on the specimens. Hence, different rehabilitation strategies were to be adopted for the recovery of seismic capacity of the selected beam-column specimens depending on the extent of damage levels. The experiment for control specimens was stopped at a stage when the load came down in the range of 60-70% of the ultimate load carrying capacity. All rehabilitated specimens were also tested with the same loading sequences as those imposed on the control specimens. Table 2 shows the details of test matrix of forty two specimens comprising of both control and rehabilitated types tested under three cyclic displacement having different characteristics.

2.5 Rehabilitating materials

A low viscous epoxy resin (combination of base and hardener) was used for injection into cracks zone. The high strength epoxy resin is a solvent free resin grout designed for grouting of crack width ranges from 0.25 to 10 mm. Micro concrete was used as a replacement material. It is a polymer modified concrete which is ready to use dry powder that requires only addition of clean water at site to produce a free-flowing non-shrink micro concrete. Bonding agent and epoxy resin base putty was used for bonding old and freshly added concrete and also for sealing all visible cracks. The properties of rehabilitating materials are presented in Table 3. Further, injections pump

Table 3 Properties of rehabilitating materials

Epoxy resin	Pot life	90 min. @ 20℃ and 40 min. @ 35℃
	Density	approx. 1050 kg/m^3
	Tensile strength	26 N/mm^2 @7days
	Flexural strength	63 N/mm^2 @7days
	Compressive strength	93 N/mm^2 @7days
Micro concrete	Compressive	40 N/mm^2 @ 7 days 50 N/mm^2 @ 28 days
Concrete bonding agent	Compressive strength	50 N/mm^2 @7 days
	Tensile strength	26 N/mm^2 @7 days
Epoxy resin based putty	Pot life	40 min. @ 27℃
	Density	1.6 g/cc
	Compressive strength	50 N/mm^2 @ 7days
	Drying time	8 hrs @ 27℃
	Fully cure	7 days @ 27℃

(hand operated) suitable for injection of low viscous epoxy were used for injecting epoxy into the cracked zone. The injection pressure is monitored through the pressure gauge. The pump has a delivery rate capacity of 0.07 L/stroke. During rehabilitation process, holes were drilled along cracks and injections packers were inserted through these holes. The injection packers are filler necks used as connection pieces between the injection device and the building component during the course of repairing of cracks. Mechanical packers (type S, length of 70 mm and dia. of 13 mm) were used in the rehabilitation works.

2.6 Rehabilitation strategies

The rehabilitation strategies were aimed to recover the lost capacity of the damaged connections up to their respective original seismic capacity. Three rehabilitation methodologies (RM) were considered depending on the degree of damages. The rehabilitation methodologies proposed in the present study were designated as RM0, RM1 and RM2. While RM0 represents patch up of surface cracks to address aesthetic issue, RM1 and RM2 correspond to fixing of real damage.

Replacement of loose concrete in the damaged portion (limited to cover concrete) by micro concrete followed by epoxy injection into the cracked zone was done in RM1. Straightened the buckled reinforcement and replacement of crushed concrete in the damaged zone (core concrete included) by micro concrete followed by epoxy injection away from the crushed zone was done in RM2. The voids created after removal of loose materials were patched or filled with micro concrete after a suitable bonding agent was applied on the cleaned surface for attaining adequate bond between old and freshly added concrete. Holes were drilled along cracks and packers were inserted through these holes. Packers served as filler neck for epoxy injection. Visible cracks were sealed and a low viscous epoxy resin was injected under high pressure into the cracked zone. Figs. 5 and 6 illustrate various steps of rehabilitation operations for typical damaged beam-column connections.

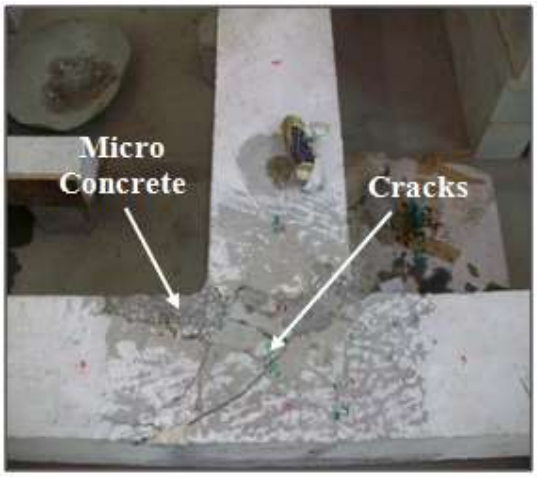

(a) Patching of spalled concrete

(b) Drilling holes along crack

(c) Installed packers and sealing of cracks

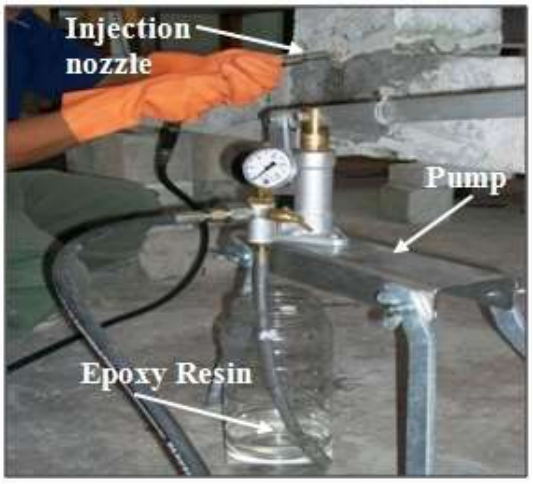

(d) High pressure epoxy injection

(e) Removing of installed packers

(f) Removing of sealing materials

Fig. 5 Step by step rehabilitation strategy (RM1)

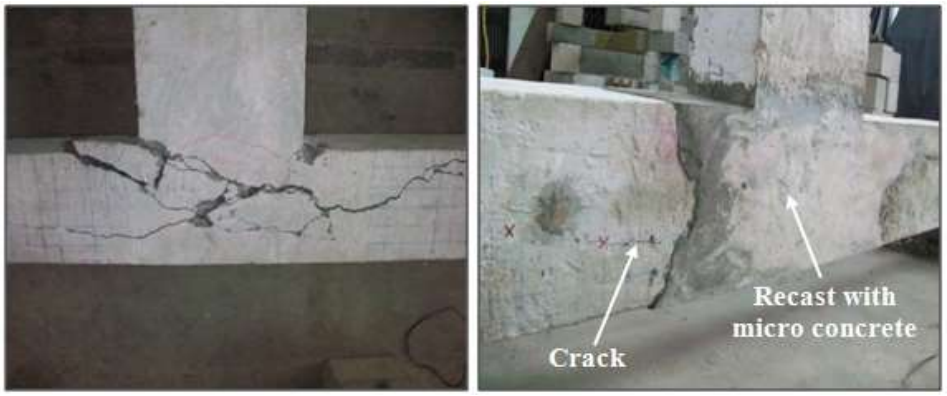

(a) Damaged specimen (b) Replacement of removed loose concrete

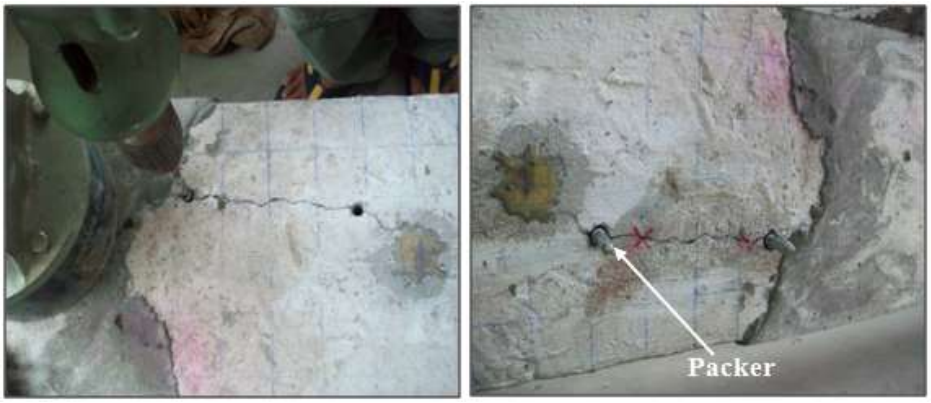

(c) Drilling holes along crack (d) Packer installation

(e) Sealing of crack (f) Epoxy resin injection

Fig. 6 Step by step rehabilitation strategy (RM2)

3. Fragility functions

Fragility functions are probability distributions that are used to indicate the probability that a component will reach or exceed a particular damage state as a function of an engineering demand parameter (EDP). The mathematical form of fragility function given by Porter *et al*. (2007b) using

lognormal distribution is defined as

$$F_i(D) = \Phi\left[\frac{ln(D/\theta_i)}{\beta_i}\right] \quad (1)$$

where *Fi* (*D*) is the conditional probability that the component will be damaged to damagestate '*i*' as a function of demand parameter (*D*), Φ denotes the standard normal (Gaussian) cumulative distribution function, θ_i denotes the median value of the probability distribution and βi denotes the logarithmic standard deviation.

In the present study, various damage states were correlated with different rehabilitation methodologies and hence, rehabilitation specific fragility functions were developed. These functions depict the probability of a suitable rehabilitation method that a damaged structural element will require for restoration of its original condition subjected to a specific level of demand. An EDP is the measure of earthquake demand on a structural component. Probability models link the EDP to the damage states and correlated to the rehabilitation method. Therefore, the probability of exceeding the damage requiring a specific rehabilitation method was modelled in the form of fragility functions.

3.1 Engineering demand parameter (EDP)

An EDP is a measure of demand imposed by events like earthquake on a structural component. In developing fragility functions, it is important to identify an EDP that most accurately and precisely relates to damage. Gulec *et al.* (2010) reported that many researchers used drift as a demand parameter. Drift angle which is defined as the ratio of beam tip displacement to the length of the beam was used as an EDP in the present study.

3.2 Identification of damage states and corresponding rehabilitation method

The extent of damage in a structural component is characterized by damage states. Damage states (DS) are linked to specific rehabilitation method. Thus, identification of the appropriate damage states is the most important steps for developing fragility functions. In this study, damage states are characterized by direct indicators of damage such as maximum concrete crack width, extent of concrete spalling, crushing and the initiation of buckling and fracture of reinforcing bars which can result in failure of the component. The damage states identified by Pagni and Lowes (2006) were used as the basis to identify the level of damage states in the current study. The specimens were damaged under cyclic loading. The same specimens were rehabilitated and then retested. Thus, the defined damage states were based on the actual observed damage from the current experimental study. The damage states and the corresponding rehabilitation methods were listed in Table 4. Corresponding drift value which is defined as the ratio of beam tip displacement to the length of the beam was also given in Table 4. These damage states were compiled from the visual examination of gradual progress of damage observed from 42 numbers of specimens tested in the structural engineering laboratory at IIT Guwahati. The damage states are presented as below:

3.2.1 Concrete cracking

Initiation, propagation and opening of concrete cracks are typical indication of damages in RC

components. DS 1.0 refers to cracking in the interface of the beam and the joint region. These cracks appeared first when demand imposed by the cyclic displacement was low. The cracks also initiated from the joint corners and progressed horizontally along the joint interface. DS 1.1 corresponds to initial cracking within the joint panel. Widths of these cracks are immeasurable. DS 1.2, 1.3 and 1.4 are subsequent stages after formation of initial cracks as shown in Fig. 7. Pagni and Lowes (2006) recommended that the development of visible, hairline cracking may be used as an indication for replacement of surface finishes. It was also suggested that rehabilitation were not required for the cracks smaller than 0.02 inch (0.5 mm). However, epoxy injection is necessary to restore the bond between the materials for crack width beyond 0.02 inch. Following these guidelines, specimens with damage states DS 1.0 to DS 1.4 were rehabilitated using RM0 method in the present study.

Further, rehabilitation was carried out using only epoxy injection for a crack width up to 2.0 mm in beam / column part of the connections and up to 5.0 mm for the joint region (DS 2.0 and DS 2.1 in Fig. 8). In case of spalling of concrete cover in the joint region, rehabilitation was done by patching of spalled concrete followed by epoxy injection into a cracked zone (DS 2.2). The damage state DS 2.3 represents further growth of damage when initial cracks formed at the joint interface widened leading to the formation of joint hinge as shown in Fig. 8. Rehabilitation of the specimens with damage states in the range DS 2.0 to DS 2.4 were carried out using the rehabilitation method RM1.

DS 3.0 indicates that the development of cracks started around the joint region first and subsequently propagated towards the column region with further increase in load as shown in Fig. 9. The crack width is beyond 2 mm in the structural elements away from joint region. Rehabilitation of specimens corresponding to these damage states were carried out with rehabilitation method- RM2, where loose concrete in the joint region was completely removed first and then the developed voids were filled with high strength concrete (micro concrete). Wider cracks, which were left on the surface of the structural elements away from the joint region, were rehabilitated with epoxy resin injection.

Table 4 Damage states and associated rehabilitation methods

ID	Damage states (*DS*)	rehabilitation methods (*RMs*)	Drift value (%)
1.0	Initial hair line cracking at the beam- column interface.	*RM0* (Cosmetic rehabilitation): Replace and restore surface finish	0 - 3
1.1	Initial hair line cracking within the joint area.		
1.2	Initial hair line cracking in the beam / column.		
1.3	Max crack width within the joint area is measurable but less than 0.5 mm.		
1.4	Max crack width in the beam / column is measurable but less than 0.5 mm.		
2.0	Crack width in the beam / column is measurable but less than 2.0 mm.	*RM1*: Epoxy resin injections in beam / column and patching of spalled cover concrete at joint area followed by use of epoxy injection.	1.4 - 7.5
2.1	Maximum crack width within the joint area is measurable but less than 5.0 mm.		
2.2	Crushing of concrete at beam-column interface edges.		
2.3	Hinge formation of beam-column interface		
2.4	Large crack of concrete surface within the joint area.		

Table 4 Continued

ID	Damage states (*DS*)	rehabilitation methods (*RMs*)	Drift value (%)
3.0	Crack width in beam / column beyond 2.0 mm.	*RM2*: Removal of damaged concrete, replacement with micro concrete and epoxy injection in cracked zone.	1.8 -7.5
3.1	Crack width within the joint region beyond 5.0 mm and crushing of concrete extend up to joint core.		
3.2	(a) Buckling of column reinforcement in zone with low shear reinforcement. (b) Buckling of beam reinforcement in zone with low shear reinforcement.		

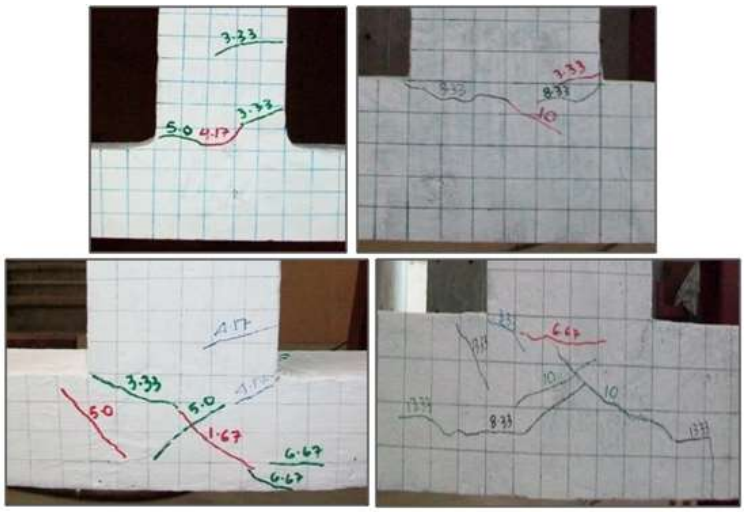

Fig. 7 Damage states in RM0 for a typical specimens

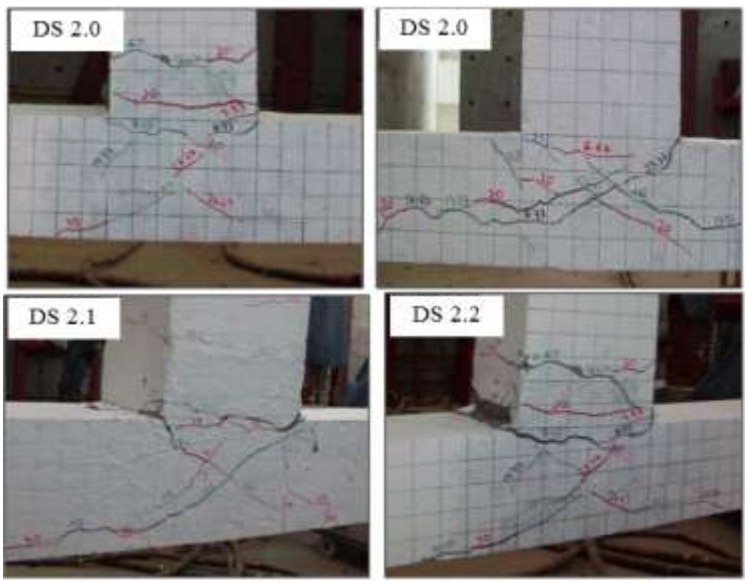

Fig. 8 Damage states in RM1 for a typical specimens

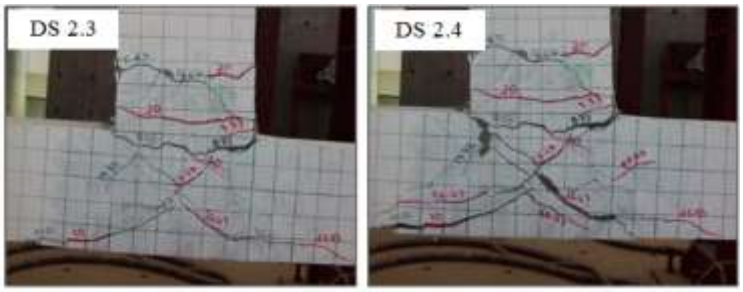

Fig. 8 Continued

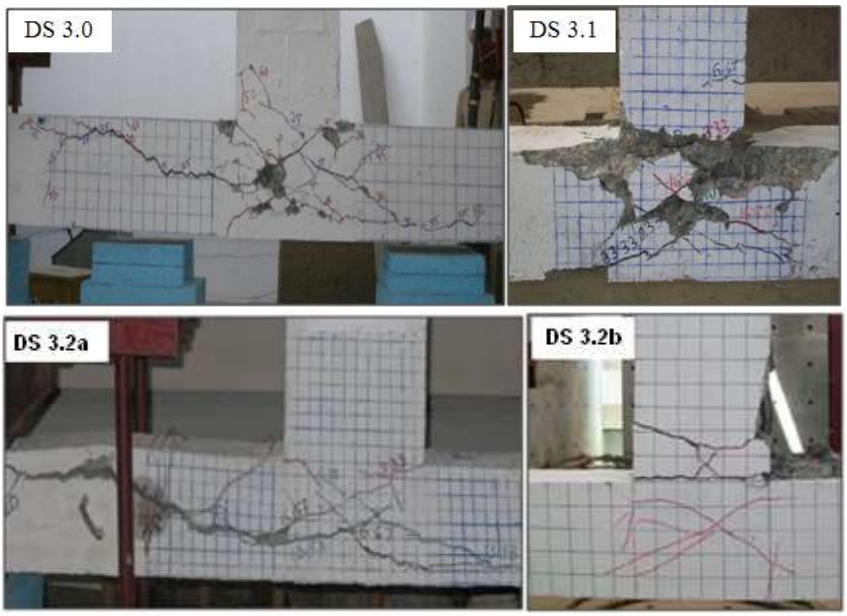

Fig. 9 Damage states in RM2 for a typical specimens

3.2.2 Crushing of concrete

Crushing of core concrete, which refers to fragmentation of concrete within the region bounded by rebars is designated as damage state DS 3.1. Crushing of concrete initiated at the edges of beam-column joint interface and cracks at the joint region were no longer measurable. DS 3.1 stands for crushing of concrete extending up to the joint core as shown in Fig. 9. Crushing and spalling of concrete thicker than the cover led to the exposure of the interior aggregate and large portion of the rebar. Damage of joint region to this extent requires complete removal of loose concrete and replacement with micro concrete for filling up the developed voided areas.

3.2.3 Joint failure

Joint failure may be characterized by a loss in lateral or gravity load carrying capacity. Loss of load carrying capacity of the order of 60-70% is considered as failure of the joint in the present study. Typically, RC components fail as a result of crushing of core concrete and buckling / fracture of reinforcing bars. The present study included three typical deficiencies where different

failure modes were observed in each deficiency type. Buckling of column reinforcement (DS 3.2a) and buckling of beam reinforcement (DS 3.2b) in the zone with low shear reinforcement are shown in Fig. 9. Beam-column connections with damage state DS 3.2 could be successfully rehabilitated using the rehabilitation method RM2.

3.3 Statistical analysis of damage data

Statistical analysis was used to develop fragility functions for beam-column connections before and after rehabilitation. Collected data were utilized to relate EDPs with RMs using standard probability distributions. The maximum likelihood method was used to fit these distributions to the data. The standard goodness-of-fit (GOF) test was performed to evaluate suitability of the considered probability distributions. Finally, most suitable distribution was identified for development of fragility functions. Four standard probability distributions were considered to model the data. The distributions considered are lognormal, Weibull, beta (Haldar and Mahadevan 2000) and gamma distribution (Hayter 2002). Each of these probability distributions was defined by two parameters that were determined using the method of maximum likelihood.

3.4 Evaluation of fragility functions

Shinozuka (2002) was the first to introduce the hypothesis testing to evaluate the fragility functions. Once the standard probability functions have been fit to the data, standard GOF tests were used to evaluate how well the probability functions model the data. Three standard GOF tests were considered, namely, Kolmogorov-Smirov (K-S), the Chi- Square (χ^2) and the Lilliefors tests.

4. Development of fragility functions for RC beam-column connections

Identification of DS based on observations made during experiment and selection of RMs for different levels of EDPs were carried out for development of rehabilitation-specific fragility functions. Cumulative frequency distribution function was obtained by plotting demand parameter in ascending order for a given damage state which was observed during experiment against $\left(\frac{i-0.5}{n}\right)$, where i is the position of the drift level within the sorted data and n is the number of samples. This derived cumulative frequency distribution functions provides the portion of the data set which does not exceed a particular value of demand. Corresponding to each rehabilitation method, four probability distribution functions were fitted to the derived cumulative frequency distribution functions in order to investigate which probability distribution would provide a better fit to the data.

4.1 Fragility functions of control specimens

Fig. 10 shows comparison of selected distribution functions to observed cumulative distribution corresponding to damage states requiring first rehabilitation method RM0. It may be concluded that each of the distributions provide an equally good fit to the data. Graphical representation of the K-S goodness-of-fit test for 5% significance levels has also been shown in Fig. 10.

The fragility functions for other levels of damage states were also developed using the selected four distribution functions. The best distribution was determined using the K-S test where the parameter (D_n) or the error was evaluated. The error was compared to a critical value (D_n^{α}) for the selected significance level of 5%. The values D_n^{α} were obtained from Table VI as furnished in Hayter (2002). Distribution providing highest probability was considered as the best fit distribution, in which the error was less than the critical value. The complete results of K-S test are furnished in Table 5. It may be concluded that each of the distribution functions provided comparable good fit to the data. However, the lognormal distribution provided the best fit among the different distributions when the critical values for each of the rehabilitation methods were compared.

Another goodness-of-fit test used in this study was the Chi-square test method. The results of Chi-square test are furnished in Table 6. The critical values were obtained from Tables II as furnished in Hayter (2002), where the result of $c_{1-\alpha,f}$ was found to be 5.991 in all the cases. The values furnished in Table 6 indicate that the Chi-Square value (error) is smaller than the Chi-Square critical value for degree of freedom 2 in all cases. However, the lognormal distributions provided best results among all distributions.

To further qualify lognormal distribution, Lilliefors goodness-of-fit tests (Lillieforss 1967) were performed. This test is a variant of the K-S test and is used when the distribution parameters are unknown. The test parameters (D_n) of the Lilliefors test corresponds to the maximum differences between the empirical cumulative distribution functions and the CDF proposed for the observed samples. Table 7 shows that lognormal distribution is acceptable in all cases studied.

The above goodness-of-fit tests show that each of the distribution functions provides comparable good fit to the data. However, the lognormal distribution provided the best fit among all the distributions. Therefore, fragility functions based on lognormal distribution were only considered for the final presentation (Fig. 11).

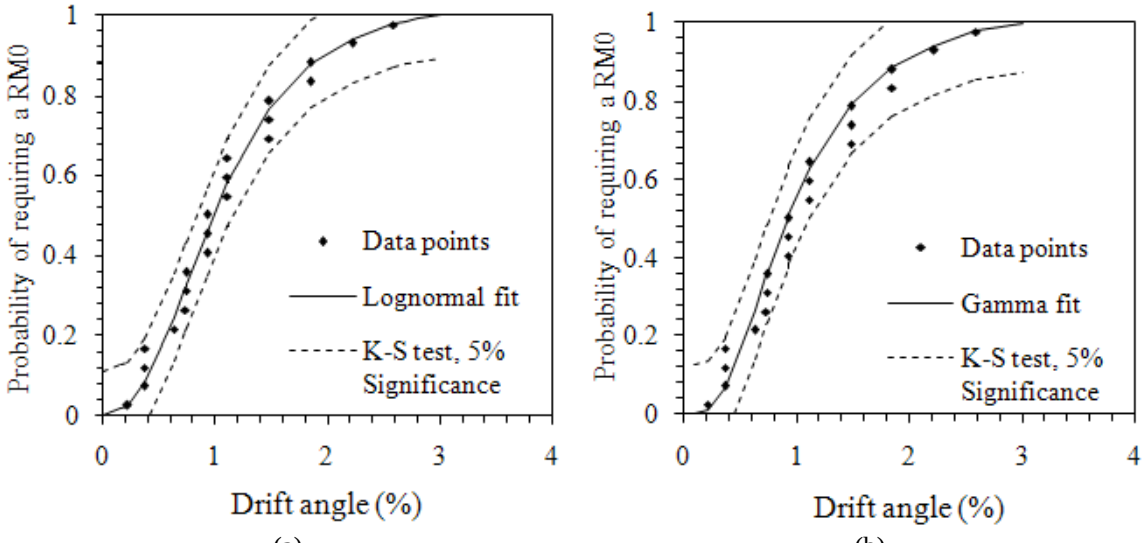

(a) (b)

Fig. 10 Fragility functions for control specimens under cosmetic rehabilitation (RM0) defined by four probability distributions: (a) lognormal (b) gamma (c) Weibull (d) beta

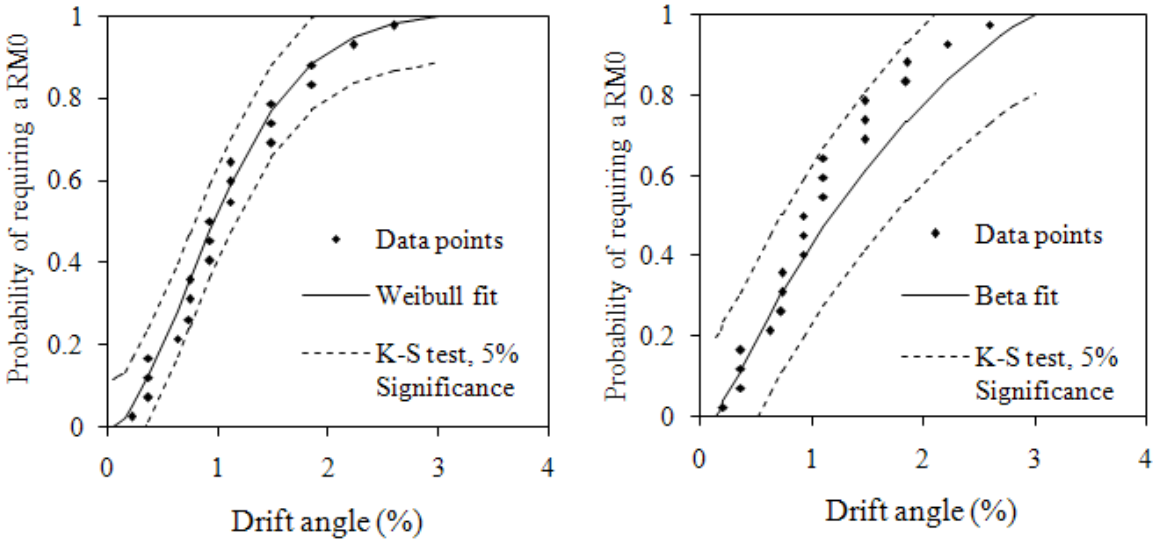

(c) (d)

Fig. 10 continued

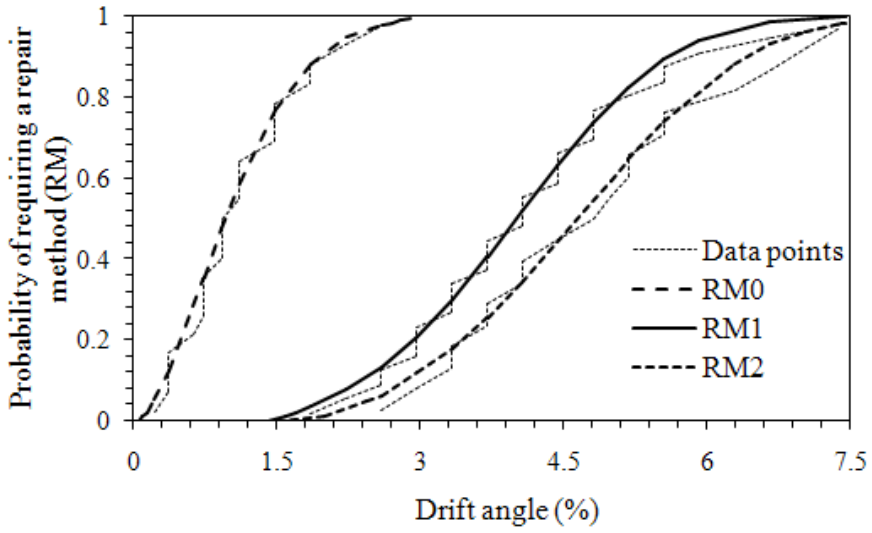

Fig. 11 Fragility functions of control specimens

Table 5 K-S test results for selected distributions for control specimens

Rehabilitation Method		RM0	RM1	RM2
Sample size	n	21	28	19
Critical Value	$\alpha = 0.05$	0.287	0.250	0.301
Lognormal distribution	Median (θ)	0.925	3.923	4.592
	Std. deviation (β)	0.617	0.328	0.298
	K-S parameter (D_n)	0.109	0.062	0.091
	$P(D_n \leq D_n^{\alpha})$	0.938	0.999	0.994

Table 5 Continued

Rehabilitation Method		RM0	RM1	RM2
Gamma distribution	Parameter (k)	3.013	9.706	11.74
Gamma distribution Weibull distribution	Parameter (λ)	0.367	0.425	0.408
	K-S parameter (D_n)	0.113	0.072	0.092
	$P(D_n \le D_n^{\alpha})$	0.922	0.997	0.993
	Parameter (k)	1.73	3.601	3.761
Weibull distribution Beta distribution	Parameter (w)	1.19	4.444	4.134
	K-S parameter (D_n)	0.125	0.082	0.095
	$P(D_n \le D_n^{\alpha})$	0.893	0.984	0.989
	Parameter (q)	0.842	2.192	0.885
Beta distribution	Parameter (r)	1.407	4.467	1.055
	Lower bound (a)	0.218	1.587	2.593
	Upper bound (b)	3.11	9.303	7.585
	K-S parameter (D_n)	0.196	0.077	0.140
	$P(D_n \le D_n^{\alpha})$	0.420	0.992	0.801

Table 6 Results of χ^2 test for selected distributions for control specimens

Distributions		RM0		RM1		RM2		Degree of freedom
		Error	*P*	Error	*P*	Error	*P*	
lognormal	$\sum_{i=1}^{m} \frac{(n_i - e_i)^2}{e_i}$	1.329	0.5145	2.659	0.448	0.055	0.814	2
Gamma		1.410	0.4942	2.755	0.431	0.024	0.877	2
Weibull		1.727	0.422	2.664	0.446	1.049	0.592	2
Beta		1.859	0.3948	2.696	0.874	0.971	0.615	2
Critical value	$c_{1-\alpha,f}$							5.991

Note: $P(D_n \le D_n^{\alpha}) = P$

Table 7 Lognormal distribution parameters of control specimens and the corresponding Lilliefors test results

Rehabilitation Group	Lognormal		Lilliefors test results			
	θ	β	D_{crit}	D_n		*Ho*
RM0	0.925	0.617	0.188	0.109		Accept
RM1	3.923	0.328	0.169	0.062	$D_n < D_{crit}$	Accept
RM2	4.592	0.298	0.195	0.091		Accept

4.2 Fragility functions of rehabilitated specimens

Fragility functions for rehabilitated specimens were also developed following the procedure adopted for control specimens and by adopting the same damage states. Fig. 12 illustrates the fragility functions developed for damaged specimens after rehabilitation.

The fragility functions for the specimens before and after rehabilitation corresponding to each

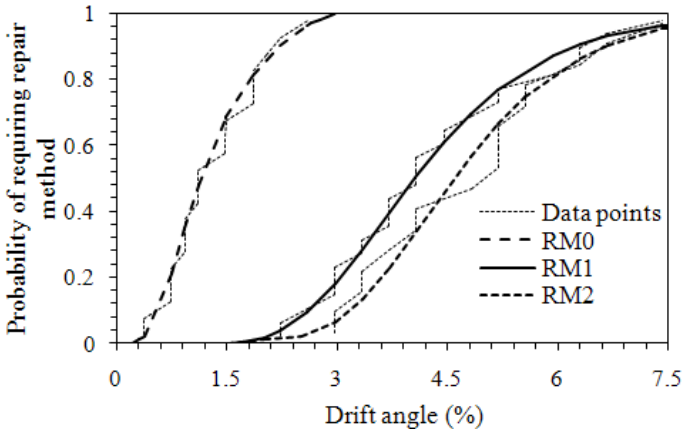

Fig. 12 Fragility functions of rehabilitated specimens

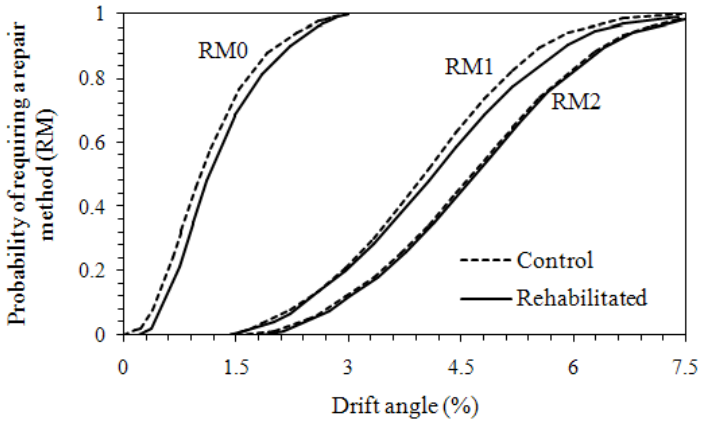

Fig. 13 Comparison of fragility functions for each rehabilitation method

rehabilitation method using lognormal distribution functions were compared in Fig. 13. Comparison of fragility functions with control specimens for each rehabilitation method showed equal or marginal improvement in probability of requiring a rehabilitation method. The close agreement of fragility functions of control and rehabilitated specimens for each rehabilitation method indicated the efficacy of adopted rehabilitation strategies.

5. Conclusions

The fragility functions of exterior RC beam-column connections before and after rehabilitation were developed considering the results of present experimental study. The data used were highly reliable as all the experiments were carried out under same control environment. Four standard probability distributions were used to model the data. Goodness-of-fit tests were employed to decide the best fit distributions. Lognormal distributions provided the most acceptable probabilities when compared for each of the rehabilitation methods.

It may be emphasized that the rehabilitating strategies were proposed based on the damage states alone. The actual field application also demands a similar approach. In view of this, the matching of fragility functions for specimens before and after rehabilitation for each rehabilitation method would provide high confidence to the field engineers for adopting similar rehabilitating strategies to address damaged RC members.

References

Applied Technology Council, ATC-13 (1985), "Earthquake damage evaluation data for California", *Applied Technology Council*, Redwood City, California.

Applied Technology Council, ATC-40 (1996), "Seismic evaluation and retrofit of concrete buildings", *Applied Technology Council*, Redwood City, California.

Aslani, H. and Miranda, E. (2005), "Fragility assessment of slab-column connections in existing non-ductile reinforced concrete buildings", *J. Earthq. Eng.*, **9**(6), 777-804.

Alsayed, S., Al-Salloum, Y., Almusallam, T. and Siddiqui, N. (2010), "Seismic response of FRP-Upgraded exterior RC beam-column joints", *J. Compos. Constr.*, ASCE, **14**(2), 195-208.

ACI 318-08 (2008), "Building code requirements for structural concrete and commentary", Farmington Hills, MI: American Concrete Institute.

Choudhury, A.M. (2010), "Study on size effect of RC beam-column connections with and without retrofitting under cyclic loading", Doctoral Thesis, Department of Civil Engineering, Indian Institute of Technology, Guwahati, India.

Federal Emergency Management Agency, FEMA (1998), *Repair of earthquake Damaged Concrete and Masonry Wall Buildings*, *FEMA* 308, 24-42.

Filiatrault, A. and Lebrun, I. (1996), "Seismic repairing of reinforced concrete joints by epoxy pressure injection technique", *ACI*, *SP*, **160**, 73-92.

Gulec, C.K., Whittaker, A.S. and Hooper, J.D. (2010), "Fragility functions for low aspect ratio reinforced concrete walls", *Eng. Struct.*, **32**(9), 2894-2901.

Haldar, A. and Mahadevan, S. (2000), *Probability, Reliability, and Statistical Methods for Engineering Design*, John Wiley & Sons, Inc.

Hayter, A.J. (2002), "Probability and statistic for engineers and scientists", Duxbury, Thompson Learning, USA.

Hadi, M.N.S. (2010), "Rehabilitating destructed reinforced concrete T- connections by steel strap", *J. Constr. Build. Mater.*, **25**(2), 851-858.

IS 456 (2000), "Plain and reinforced concrete - Code of Practice", *Bureau of Indian Standard*, New Delhi.

IS 13920 (1993), "Ductile detailing of reinforced concrete structures subjected to seismic forces - Code of Practice", Bureau *of Indian Standard*, New Delhi.

IS: 12269 (1987), "Specification for OPC-53 grade cement", *Bureau of Indian Standard,* New Delhi.

IS: 10262 (2009), "Guidelines for concrete mix design proportioning (CED 2: Cement and Concrete)", *Bureau of Indian Standard*, New Delhi.

IS: 2386a (1963), "Methods of test for aggregates for concrete - Part 1: Particle size and shape", *Bureau of Indian Standard*, New Delhi.

IS: 2386b (1963), "Methods of Test for aggregates for concrete - Part 3: Specific gravity, Density, Voids, Absorption and Bulking", *Bureau of Indian Standard*, New Delhi.

IS: 432 (1) (1982), "Specification for mild steel and medium tensile steel bars and hard-drawn steel wire for concrete reinforcement: Part I Mild steel and medium tensile steel bars", *Bureau of Indian Standard*, New Delhi.

IS: 1608 (1995), "Mechanical testing of metals - tensile testing", *Bureau of Indian Standard*, New Delhi.

Jeon, J., Lowes, L.N., DesRoches, R. and Brilakis, I. (2015), "Fragility curves for non-ductile reinforced concrete frames that exhibit different component response mechanisms", *Eng. Struct.*, **85**, 127-143.

Karayannis, C.G., Chalioris, C.E. and Sideris, K.K. (1998), "Effectiveness of RC beam-column connection repair using epoxy resin injections", *J. Earthq. Eng.*, **2**(2), 217-240.
Karayannis, C.G., Chalioris, C.E. and Sirkelis, G.M. (2008a), "Local retrofit of exterior beam-column joints using thin RC jackets-An experimental study", *J. Earthq. Eng. Struct. Dyn.*, **37**(5), 727-746.
Karayannis, C.G. and Sirkelis, G.M. (2008b), "Strengthening and rehabilitation of RC beam-column joints using C-FRP jacketing and epoxy resin injection", *J. Earthq. Eng. Struct. Dyn.*, **37**(5), 769-790.
Lignos, D., Kolios, D. and Miranda, E. (2010), "Fragility assessment of reduced beam section moment connections", *J. Struct. Eng*, **136**(9), 1140-1150.
Lilliefors, H.W. (1967), "On the K-S Test for normality with mean and variance unknown", *J. Am. Statistic. Assoc.*, **62**(318), 399-402.
Marthong, C., Dutta, A. and Deb, S.K. (2013), "Seismic rehabilitation of RC exterior beam-column connections using epoxy resin injection", *J. Earthq. Eng.*, **17**(3), 378-398.
Mosalam, K.M., Ayala, G., White, R.N. and Roth, C. (1997), "Seismic fragility of LRC frames with and without masonry infill walls", *J. Earthq. Eng.*, **1**(4), 693-719.
Marthong, C. and Marthong, S. (2016), "An experimental study on the effect of PET fibers on the behavior of exterior RC beam-column connection subjected to reversed cyclic loading", *Struct. J.*, **5**, 175-185.
Mukherjee, A. and Joshi, M. (2005), "FRPC reinforced concrete beam-column joints under cyclic excitation", *Compos. Struct.*, **70**(2), 185-199.
Pagni, C.A. and Lowes, L.N. (2006), "Fragility functions for older reinforced concrete beam-column joints", *Earthq. Spectra*, **22**(1), 215-238.
Porter, K., Kennedy, R. and Bachman, R. (2007a), "Creating fragility functions for performance-based earthquake engineering", *Earthq. Spectra*, **23**(2), 471-489.
Porter, K., Hamburger, R. and Kennedy, R. (2007b), "Practical development and application of fragility functions", *Struct. Eng. Res. Front.*, 1-16.
Ramamoorthy, S.K. (2006), "Seismic fragility estimates for reinforced concrete framed buildings", Doctoral Thesis, Department of Civil Engineering, Graduate Studies of Texas A&M University, United States.
Shinozuka, M., Kim, S., Kushiyama, S. and Yi, J. (2002), "Fragility curves of concrete bridges retrofitted by column jacketing", *Eng. Eng. Vib.*, **1**(2), 195-205.
Singhal, A. and Kiremidjian, A.S. (1996), "Method for probabilistic evaluation of seismic structural damage", *J. Struct. Eng.*, **122**(12), 1459-1467.
Tsonos, A.G. (2001), "Seismic repairing of reinforced concrete joints by removal and replacement technique", *Eur. Earthq. Eng.*, **3**, 29-43.
Yamazaki, F. and Murao, O. (2000), "Vulnerability functions for Japanese buildings based on damage data from the 1995 Kobe earthquake", *Implication of recent earthquakes on seismic risk: Series on Innovation and Construction*, Imperial College Press, London, **2**, 91-102.
Yurdakul, O. and Avsar, O. (2015), "Structural repairing of damaged reinforced concrete beam- column assemblies with CFRPs", *Struct. Eng. Mech.*, **54**(3), 521-543.

CC